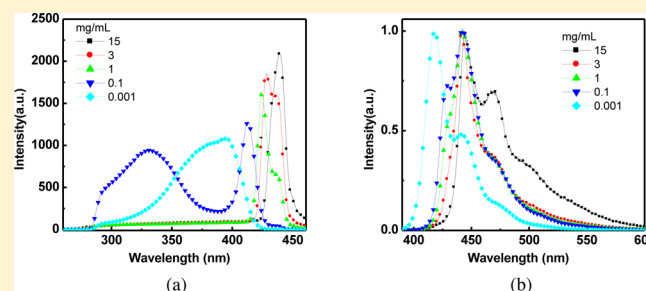


## H- and J-Aggregation of Fluorene-Based Chromophores

Yonghong Deng,<sup>\*,†,‡</sup> Wen Yuan,<sup>†</sup> Zhe Jia,<sup>†</sup> and Gao Liu<sup>\*,†</sup><sup>†</sup>Environmental Energy Technologies Division, Lawrence Berkeley National Laboratory, 1 Cyclotron Road, Berkeley, California 94720, United States<sup>‡</sup>School of Chemistry and Chemical Engineering, South China University of Technology, Wushan Road, Tianhe District, Guangzhou 510640, People's Republic of China

## S Supporting Information

**ABSTRACT:** Understanding of H- and J-aggregation behaviors in fluorene-based polymers is significant both for determining the origin of various red-shifted emissions occurring in blue-emitting polyfluorenes and for developing polyfluorene-based device performance. In this contribution, we demonstrate a new theory of the H- and J-aggregation of polyfluorenes and oligofluorenes, and understand the influence of chromophore aggregation on their photoluminescent properties. H- and J-aggregates are induced by a continuous increasing concentration of the oligofluorene or polyfluorene solution. A relaxed molecular configuration is simulated to illustrate the spatial arrangement of the bonding of fluorenes. It is indicated that the relaxed state adopts a  $2_1$  helical backbone conformation with a torsion angle of  $18^\circ$  between two connected repeat units. This configuration makes the formation of H- and J-aggregates through the strong  $\pi$ - $\pi$  interaction between the backbone rings. A critical aggregation concentration is observed to form H- and J-aggregates for both polyfluorenes and oligofluorenes. These aggregates show large spectral shifts and distinct shape changes in photoluminescent excitation (PLE) and emission (PL) spectroscopy. Compared with "isolated" chromophores, H-aggregates induce absorption spectral blue-shift and fluorescence spectral red-shift but largely reduce fluorescence efficiency. "Isolated" chromophores not only refer to "isolated molecules" but also include those associated molecules if their conjugated backbones are not compact enough to exhibit perturbed absorption and emission. J-aggregates induce absorption spectral red-shift and fluorescence spectral red-shift but largely enhance fluorescence efficiency. The PLE and PL spectra also show that J-aggregates dominate in concentrated solutions. Different from the excimers, the H- and J-aggregate formation changes the ground-state absorption of fluorene-based chromophores. H- and J-aggregates show changeable absorption and emission derived from various interchain interactions, unlike the  $\beta$  phase, which has relatively fixed absorption and emission derived from an intrachain interaction.



## 1. INTRODUCTION

Polyfluorenes, as one of the typical blue-light-emitting polymers for OLEDs, attract great attention due to their high quantum yield and thermal stability.<sup>1–3</sup> The fluorene structure is composed of a biphenyl unit bridged with a methylene unit at the 9 position. The protons on the methylene unit can be substituted by alkyl chains to improve the polymer solubility, without significantly altering the band gap of the material. Polyfluorenes show excellent absorbance and luminescent properties due to their partial conjugation along the chain. The photophysical features of polyfluorenes are related to their phase behaviors,<sup>4–9</sup> the presence of fluorenone defects,<sup>10,11</sup> excimer formation, and chromophoric aggregation.<sup>12,13</sup>

Polyfluorene chromophoric aggregation gives two forms: polymer chain association and chromophoric aggregation, such as H- and J-aggregates.<sup>14</sup> Previous researchers have investigated the aggregation of polyfluorene solutions and films, but they referred to the term "aggregation" as an association of partially aligned polymer chains and not necessarily as an assembly of chromophores with distinct absorption features in the ground

state such as H- and J-aggregates.<sup>15</sup> H- or J-aggregates are formed through the  $\pi$ - $\pi$  interaction of the chromophores with close interchromophore spacing and strong coupling. Because of those early stage investigations, the  $\pi$ - $\pi$  aggregation has been named according to the relative position of the aggregate absorption band to the molecular absorption band (M-band) with "isolated" chromophore. H-aggregation denotes the aggregation showing a blue-shifted band (hypsochromic band or H-band) to the M-band, whereas J-aggregation refers to the aggregation exhibiting a red-shifted band. The large spectral shifts and distinct changes in band shapes can be rationalized on the basis of the exciton model and screening model.<sup>16–20</sup> Because of  $\pi$ - $\pi$  interaction of two conjugated chromophoric groups, the excited chromophores split into two energy levels: the upper level and the lower level. For H-aggregation, it is the upper level which corresponds to the allowed transition, and

Received: October 19, 2014

Revised: November 16, 2014

Published: November 17, 2014

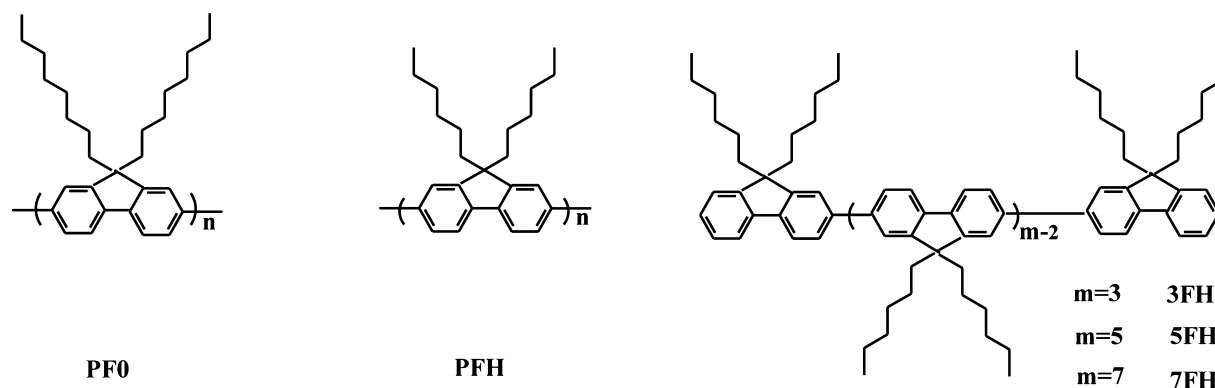


**Figure 1.** Chemical structure and abbreviated nomenclature of the polyfluorenes and oligofluorenes.

thus, there is an absorbance spectral blue-shift. Transitions to the lower level are forbidden; hence, any fluorescence, following relaxation from the higher to the lower level, is very weak and will resist any electroluminescence. For J-aggregation, it is the lower level corresponding to the allowed transition, and accordingly, there is an absorbance spectral red-shift. J-aggregation favors fluorescence; therefore, it is beneficial to electroluminescence.<sup>21</sup> As the  $\pi$ - $\pi$  interaction is accompanied by significant color and luminescence variations, the chromophoric aggregation effect has been extensively investigated in the fields of photoresponsive materials,<sup>22–28</sup> photographic science and engineering, textile coloring,<sup>29,30</sup> biophotonics,<sup>31,32</sup> and linear and nonlinear optics.<sup>33–37</sup> In this work, we first reported the H- and J-aggregation behavior of fluorene-based chromophores.

In this paper, we discuss H- and J-aggregation behaviors of polyfluorenes and oligofluorenes caused by the strong current interest in aggregation phenomena and their effects on the emissive properties of conjugated polymers. For polyfluorenes and oligofluorenes with high concentration, the existing status of chromophores is a mixture of “isolated” chromophores, H- and J-aggregates of chromophores. The formation of H- and J-aggregates is dependent on the alignments of the coplanar backbones of polyfluorenes and oligofluorenes. It is reported that H-aggregation of conjugated polymers favors photovoltaic devices because of the necessary separation of electrons and holes, and J-aggregation favors fluorescence and is beneficial to electroluminescence of OLED.<sup>21,38,39</sup> Therefore, investigating H- and J-aggregation behavior of polyfluorenes is important for both a better understanding of polyfluorene photophysics and a better design of polyfluorene-based photoelectronic devices.

## 2. EXPERIMENTAL SECTION

**Characterization.** <sup>1</sup>H NMR spectra were obtained on a Bruker AV-300 spectrometer. Gel permeation chromatography (Waters Breeze system) was used to determine the molecular weights against polystyrene standards. A Lambda 900 UV/vis/NIR spectrometer from PerkinElmer was used for absorbance spectroscopy over a wavelength range from 200 to 800 nm. Quartz cuvettes were used for measurements in solutions. A Hitachi F7000 fluorescence spectrofluorometer was used for photoluminescent excitation (PLE) and emission (PL) spectroscopy. The PLE and PL spectra were measured using a xenon lamp as the light source at room temperature.

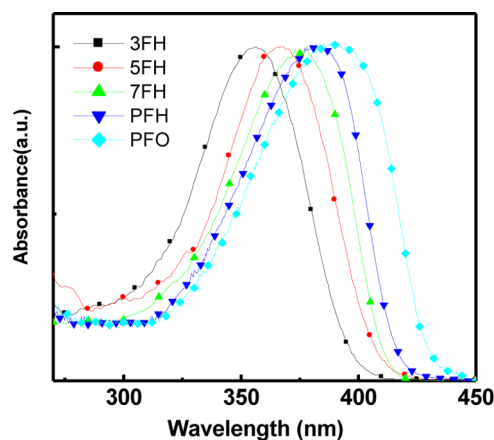
**Materials.** Poly(9,9-di-*n*-octyl-2,7-fluorene) (PFO) used here was purchased from American Dye Source, Quebec, Canada (Catalog No. ADS129BE). The number-average

molecular mass was 147 000 kg/mol (polydispersity index PDI = 3). Poly(9,9-di-*n*-hexyl-2,7-fluorene) (PFH) was synthesized in our group, and the synthesis details are given in the Supporting Information. The number-average molecular weight of PF6 was 3353 (polydispersity index PDI = 1.68). Oligofluorenes with different monomer units, such as 9,9-di-3-hexyl-2,7-fluorene (3FH), 9,9-di-5-hexyl-2,7-fluorene (5FH), and 9,9-di-7-hexyl-2,7-fluorene (7FH), were synthesized according to the ref 21. Other reagents were purchased from Sigma-Aldrich Co. and used without further purification.

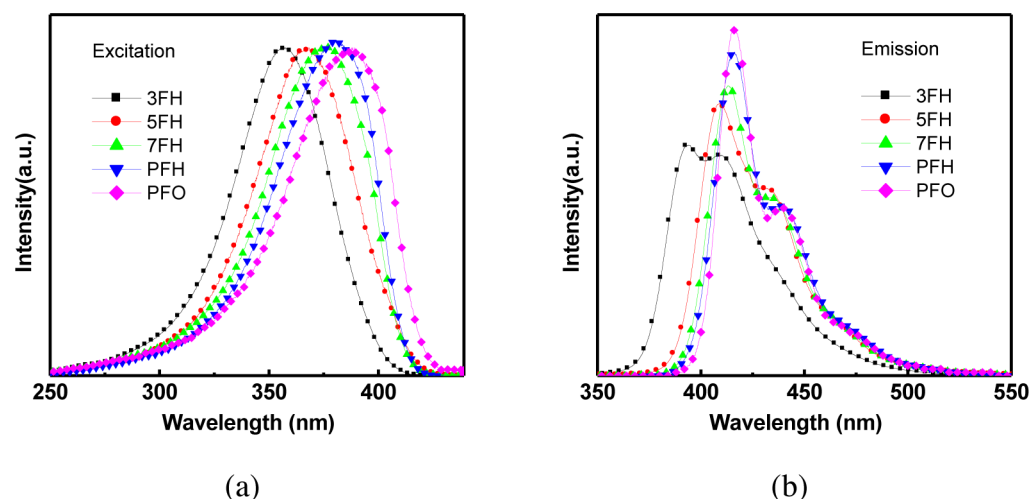
**Sample Preparation.** The PFO, PFH, 3FH, 5FH, and 7FH were dissolved in chloroform to obtain clear solutions with various concentrations in the range of  $10^{-6}$  to 15 g/L. Every original sample was kept stirring for 20 min and then put aside for 72 h. The diluted solutions were kept for at least 20 min before fluorescence and absorption measurement.

## 3. RESULTS AND DISCUSSION

**3.1. Photoluminescent Excitation and Emission.** The structures of oligofluorenes and polyfluorenes are given in Figure 1. 3FH, 5FH, and 7FH are 9,9-di-*n*-hexyl-2,7-fluorenes with 3, 5, and 7 monomer repeating units, respectively. PFH is poly(9,9-di-*n*-hexyl-2,7-fluorene) with Mn of 3353 kg/mol (PDI = 1.68), and PFO is poly(9,9-di-*n*-octyl-2,7-fluorene) with Mn of 147 000 kg/mol (PDI = 3.0). Both oligofluorenes and polyfluorenes can be completely dissolved in chloroform with clear solutions. Figure 2 shows the UV-vis absorption spectra of the oligofluorenes and polyfluorenes in chloroform. The



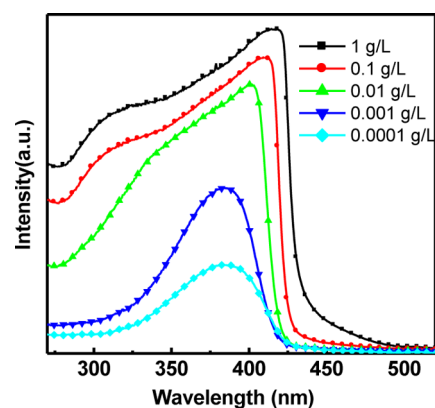
**Figure 2.** UV-vis absorption spectra of oligofluorenes and polyfluorenes in chloroform with concentration of  $10^{-6}$  g/L.



**Figure 3.** (a) PLE spectra (monitored at the maximum emission) and (b) PL spectra (excited at the maximum absorption) of the polyfluorenes and oligofluorenes in chloroform with a concentration of  $10^{-6}$  g/L.

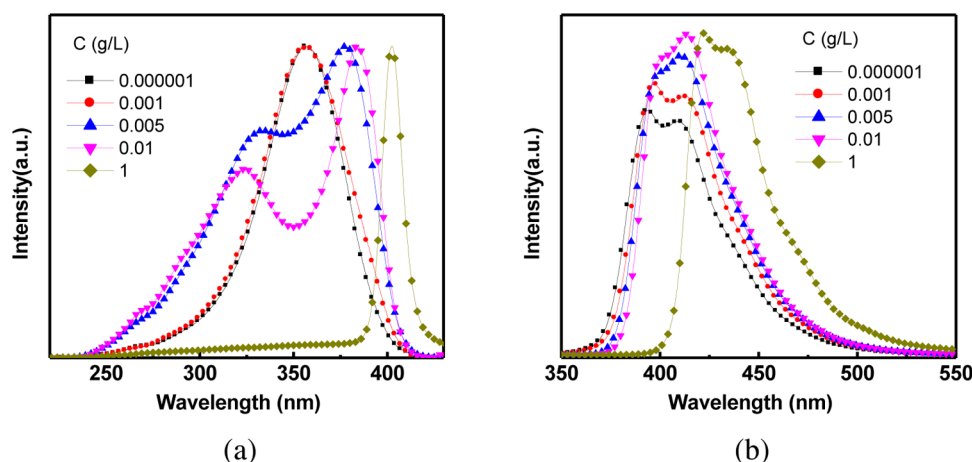
concentration was chosen to be  $10^{-6}$  g/L to avoid intermolecular interactions in solution. The maximum absorption peak ( $\lambda_{\max}$ ) of the oligofluorene is red-shifted with increasing number ( $n$ ) of fluorene units, consistent with the results in the literature.<sup>40–43</sup> The red-shifted phenomenon can be interpreted as a result of enhanced coupling interaction. Although there is a great difference in molecular weight between PFH and PFO, their absorption spectra are similar due to a similar effective conjugated length. Here the effective conjugated length of the polyfluorenes is defined as the minimum number of bonded monomer units necessary to produce saturation in the optical and electronic properties.<sup>41</sup> Although PFH and PFO have different numbers of methylene units in the substituted groups at the 9 position of the polyfluorene backbones, this does not significantly change the absorption property of the material. Compared with 3HF or 5FH, the polyfluorenes and 7FH show a steeper absorption edge on the long wavelength side than on the short wavelength side. It may be caused by an inhomogeneous intrachain coupling interaction. Figure 3 shows the corresponding photoluminescent excitation (PLE) and photoluminescent emission (PL) spectra of the oligofluorenes and polyfluorenes in chloroform. The excitation spectra (Figure 3a), monitored at maximum emission, are almost the same as the corresponding UV–vis absorption spectra. The emission spectra were excited at the corresponding energy of maximum absorption. As Figure 3b shows, three well-resolved emission fluorene bands are observed in the oligofluorenes and the homopolymers, which are assigned to the 0–0, 0–1, and 0–2 intrachain singlet transitions.<sup>44</sup> The relative intensity of the 0–0 transition increases, while that of the 0–1 transition decreases with the increase of effective conjugation. The results are consistent with the ones in the literature.<sup>41–43</sup>

Figure 4 displays the UV–vis absorption spectra of 3FH in chloroform with different concentrations. The absorption spectrum has little change with the increase of concentration when the concentration is lower than 0.001 g/L. As the concentration increases, the absorption spectrum of 3FH becomes broader. It is also interesting to observe that these spectra show a steeper absorption edge on the long wavelength side than on the short wavelength side. Figure 5 shows the PLE and PL emission spectra of 3FH in chloroform with different



**Figure 4.** UV–vis absorption spectra of 3FH with different concentrations.

concentrations. The emission spectra were excited at 353 nm, and the excitation spectra were monitored at 420 nm. When the concentration is changed from  $10^{-6}$  to  $10^{-3}$  g/L, the absorbance and emission bands of 3FH have no spectral shift. The  $\pi$ – $\pi^*$  transition peak is 353 nm in the PLE spectra, and three emission bands at 390, 408, and 430 nm are observed in the PL spectra. When the concentration reaches 0.001 g/L, the PLE spectra start to become broad. When the concentration is 0.005 g/L, the  $\lambda_{\max}$  at 353 nm splits into two peaks: One is at 333 nm, and the other is at 377 nm. By slightly increasing the concentration from 0.005 to 0.01 g/L, the peak at 333 nm blue-shifts to 325 nm, and the peak at 377 nm red-shifts to 382 nm. With the concentration further increasing, the peak at the short-wavelength side becomes more and more weak, but the peak at the long-wavelength side becomes more and more strong. When the concentration reaches 1 g/L, the peak at the long-wavelength side becomes dominant and shows a  $\lambda_{\max}$  value at 408 nm, but the peak at the short-wavelength side disappears and a broad band appears spanning from 220 to 380 nm. Obviously, the excitation spectra of 3FH are different from the corresponding UV–vis absorption spectra when the concentration is above 0.001 g/L. For the corresponding PL emission spectra, the relative intensity of the 0–0 transition decreases, whereas the relative intensity of the 0–1 transition increases along with the increase of concentration. Meanwhile, PL



**Figure 5.** (a) PLE spectra (monitored at 420 nm) and (b) PL spectra (excited at 356 nm) of 3FH with various concentrations.

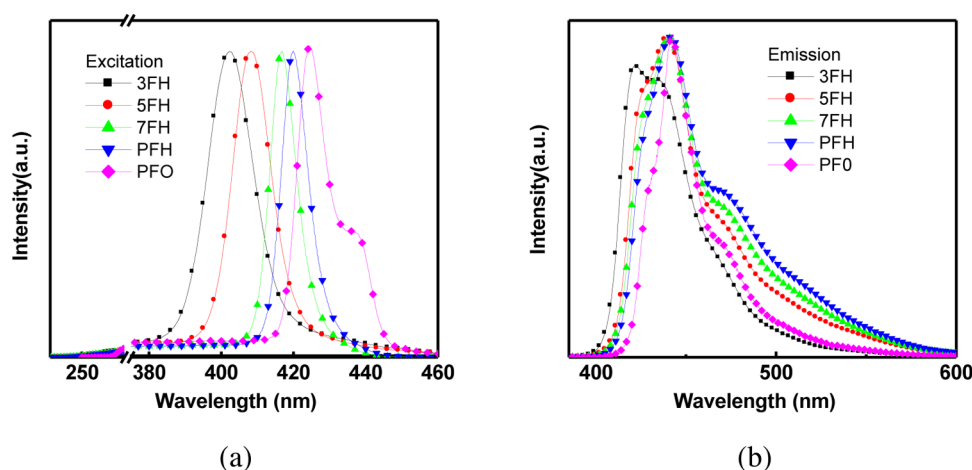


**Figure 6.** (a) PLE spectra (monitored at the maximum emission) and (b) PL spectra (excited at the maximum absorption) of the polyfluorenes and oligofluorenes in chloroform with a concentration of 1 g/L.

spectra show a spectral red-shift with the concentration increase.

5FH, 7FH, PFH, and PFO have a similar chromophoric aggregation behavior, induced by increasing solution concentrations. Figure 6 shows the PLE and PL of the oligofluorenes and polyfluorenes in chloroform with concentration of 1 g/L. When the concentration rose from  $10^{-6}$  to 1 g/L, the PLE spectrum of the fluorene-based chromophores had a very clear spectral red-shift due to the strong interchain  $\pi$ - $\pi$  interaction between conjugated chromophores. The PLE spectrum has a narrow absorption peak on the long-wavelength side and an additional tail on the short-wavelength side, demonstrating complex aggregates coexisted in this system. The PLE of 1 g/L PFO in chloroform has an additional absorption peak located at 437 nm due to the formation of the  $\beta$  phase. As shown in Figure 6b, with the concentration changed from  $10^{-6}$  to 1 g/L, PL emission shows spectral red-shift significantly, together with a great change in spectral shape. This phenomenon also indicates that chromophoric aggregation occurs in the oligofluorene and polyfluorene system, induced by increasing solution concentrations.

**3.2. H-Aggregation and J-Aggregation. Molecular Configuration.** To understand the configuration of oligofluorenes and polyfluorenes, these molecules are simulated by the semiempirical NDDO-AM1 Hamiltonian.<sup>45</sup> Figure 7 shows the

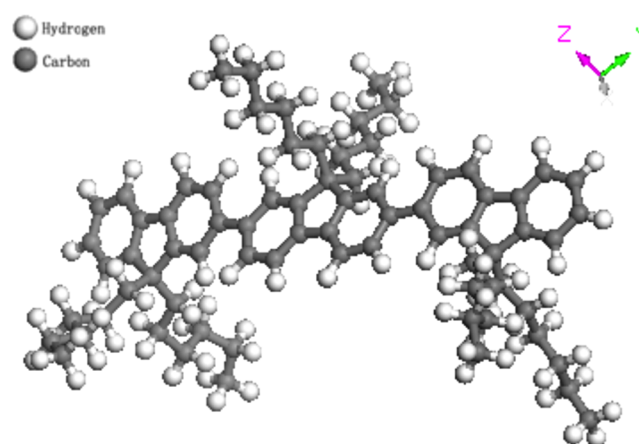


**Figure 7.** Molecular configuration for the relaxed structure of 3FH.

relaxed structure of 3FH, which is selected to illustrate the spatial arrangement of the bonding of fluorenes. A torsion angle of  $18^\circ$  is found between the backbone rings of two connected repeating units. The two substituted hexyl groups at the 9 position display a symmetric zigzag conformation, and are almost perpendicular to the backbone plane. The optimized backbone geometry of these oligofluorenes and polyfluorenes is an approximate  $2_1$  helix conformation (Figure 8) with a torsion



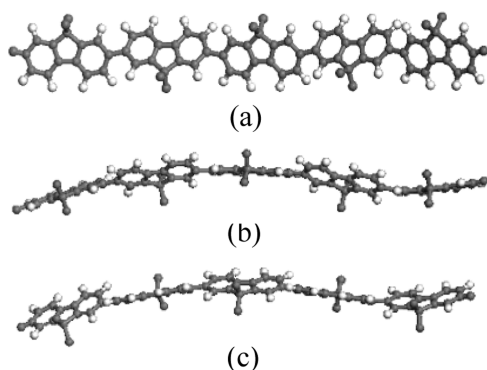


**Figure 8.** A simplified relaxed structure of the backbone rings to illustrate the bonding of fluorene units: (a) a full-face profile; (b) a side-face profile; (c) another side-face profile obtained by rotating part b at an angle around 18°.

angle around 18°, similar to the extended polyfluorene conformation proposed by Grell et al.<sup>5</sup> The oligofluorenes and polyfluorenes with this type of ground state configuration tend to form H-aggregates and J-aggregates because of the strong  $\pi$ – $\pi$  interaction within the coupling backbone rings.

In McRae's theory, the formation of H- or J-aggregates is dependent on the aligned angle between transitional moments and the center-to-center axis of the two chromophores (Figure 9). The J-aggregate has an aligned angle smaller than 54.7°,

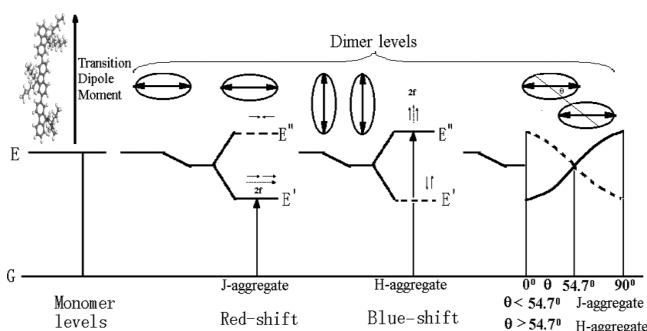


**Figure 9.** Classification of possible transitions for the H-aggregate and J-aggregate of two coupled molecules.

while the H-aggregate has an angle larger than 54.7°.<sup>17</sup> The oligofluorenes and polyfluorenes can form J-aggregates and H-aggregates, depending on solution conditions, which can result in different optical physical properties. Figure 10 shows a simple model of a “dimer” (a double-chromophore aggregate) formed from two 3FH chromophores. 3FH is selected to demonstrate the spatial arrangement of J-aggregates and H-aggregates for all the oligofluorenes and polyfluorenes. Here, H-

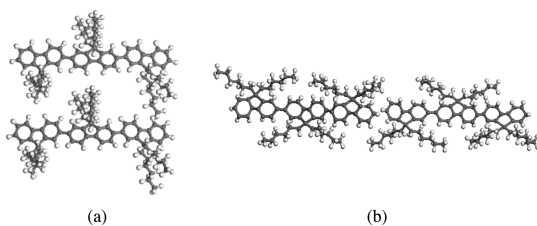


**Figure 10.** Simplified spatial arrangement of (a) the H-aggregate and (b) the J-aggregate formed from two 3FH molecules.

or J-aggregates are displayed with two extreme cases. “H-aggregate” is represented by the parallel-type aggregates with an alignment angle of 90°, and “J-aggregate”, by the bottom-to-head alignment of the chromophores with an angle of 0°.

**Energy Shift.** In accordance with the theory of molecular excitons proposed by Kasha et al.,<sup>46</sup> the energy shift between the “isolated” chromophore band ( $E_s$ ) and the chromophoric aggregate ( $E_{agg}$ ) can be approximately expressed as follows:

$$\Delta E = E_{agg} - E_s \propto \frac{|M|^2}{r^3} (\cos \alpha + 3 \cos^2 \theta) \quad (1)$$

Therefore, the energy shift ( $\Delta E$ ) of H- and J-aggregates is affected by the transition moment ( $M$ ), the center-to-center distance between two molecules ( $r$ ), the angle between polarization axes for the component absorbing units ( $\alpha$ ), and the angle made by the polarization axes of the unit molecule with the line of molecular centers ( $\theta$ ).

The formation of H- and J-aggregates induces the significant spectral shifts and distinct shape change with increasing concentration, as shown in Figure 5. When the concentration is in the range of  $10^{-6}$ – $10^{-3}$  g/L, the PLE and PL spectra of 3FH show no perceptible change with the concentration change. Therefore, these 3FH molecules can be regarded as “isolated” chromophores. The maximum absorption of the “isolated” chromophores is located at 353 nm, and the corresponding emission spectrum shows transition peaks at 390, 408, and 430 nm. Here, the emission peaks are obtained by peak-fitting with the Gaussian method, as shown in Figure S1 in the Supporting Information. When the concentration is in the range of  $10^{-3}$ –1 g/L, both PLE and PL spectra have a significant spectral shift with concentration, together with a great change in spectral shape. The difference between the UV–vis absorption spectra and PLE spectra becomes obvious. Here, the critical aggregation concentration of 3FH in chloroform, at which “isolated” chromophores start to form H- or J-aggregates, can be determined to be  $10^{-3}$  g/L. It is worth mentioning that the PLE spectrum exhibits a selected absorption when monitored at a specific emission wavelength. The UV–vis absorption spectrum is different from the PLE spectrum when H- and J-aggregation occurred in this system. The absorption spectrum displays the full wavelength without selection. As we know, J-aggregation favors fluorescence and improves fluorescent quantum efficiency, while H-aggregation inhibits fluorescence and reduces fluorescent quantum efficiency. Therefore, the PLE spectrum only exhibits those absorptions that make contribution to the emission at a specific wavelength, which results in a PLE spectrum that may show dominant J-aggregates, even though H- and J-aggregates contribute equally.

There exists dynamic equilibrium between “isolated” chromophores and precursor aggregates when the concentration is near 0.001 g/L. Part of the “isolated” 3FH chromophores form aggregates when the concentration is above 0.001 g/L. When the concentration reaches 0.005 g/L, the absorption peak at 353 nm decreases, and two new absorption peaks appear at 330 and 377 nm, indicating that some of the “isolated” 3FH chromophores align themselves to form H- ( $\lambda_{max} = 333$  nm) and J-aggregates ( $\lambda_{max} = 377$  nm). The corresponding emission spectrum red-shifts slightly. The emission ratio of the second peak to the first peak increases, indicating that the H- and J-aggregates cause new emission peaks on the long wavelength side. When the concentration is at 0.01 g/L, the  $\lambda_{max}$  of H-aggregates blue-shifts to 325 nm and

Table 1. Spectral Parameters of PLE and PL Spectra for Oligofluorenes and Polyfluorenes with Two Concentrations

samples		excitation $\lambda_{\text{max}}$ (nm)		$\Delta E_{\text{ex}}$	emission $\lambda$ (nm) (the first peak)		
		$C = 10^{-6}$ g/L	$C = 1$ g/L		$C = 10^{-6}$ g/L	$C = 1$ g/L	$\Delta E_{\text{em}}$
oligofluorene	3FH	356	408	52	398	421	23
	5FH	367	410	43	409	423	14
	7FH	378	421	43	413	423	10
polyfluorene	PFH	383	424	41	414	424	10
	PFO	385	426	41	417	427	10

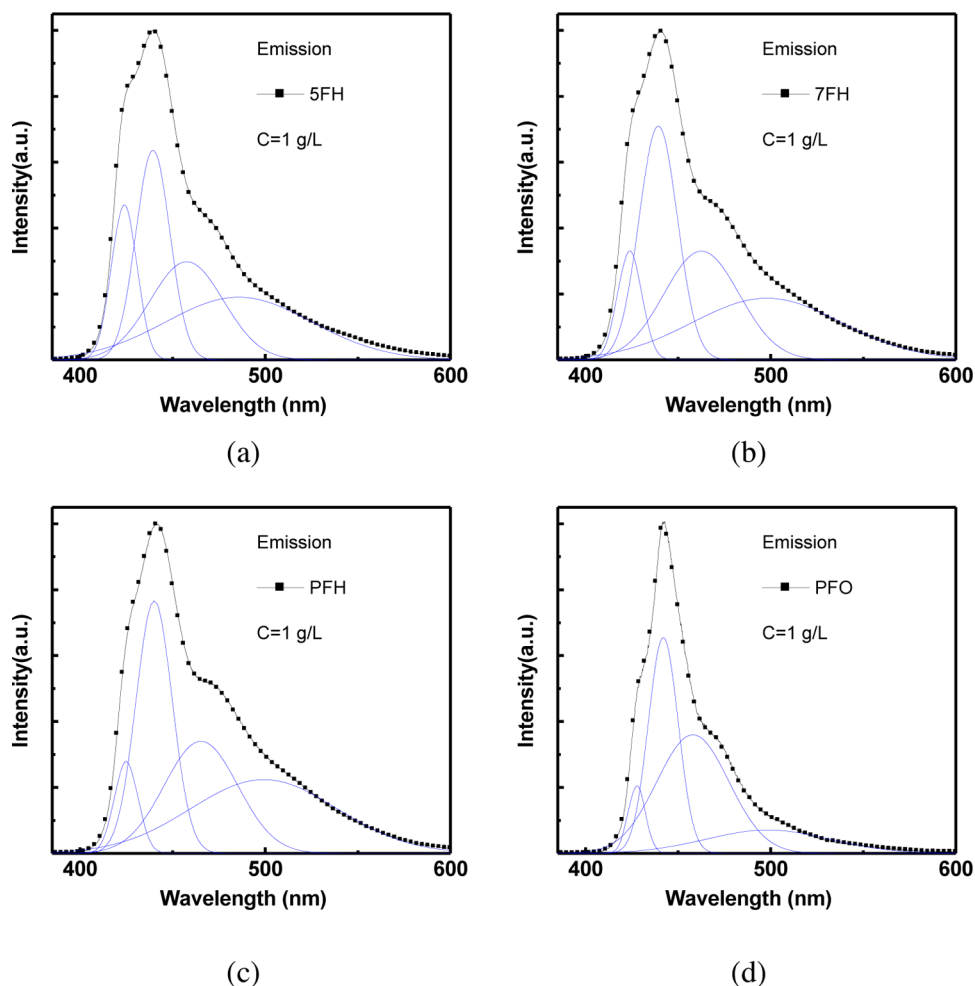


Figure 11. Decomposition of the PL spectra into constituent peaks by the peak-fitting method: (a) 5FH; (b) 7FH; (c) PFH; (d) PFO.

the  $\lambda_{\text{max}}$  of J-aggregates red-shifts to 382 nm. According to eq 1, this energy shift originates from enhanced H-aggregation and J-aggregation. The absorption intensity of the J-aggregates increases, while that of the H-aggregates decreases gradually with the concentration increases, indicating that more and more J-aggregates contribute to the corresponding emission at 420 nm. When the concentration reaches 1 g/L, the PLE peak of J-aggregates becomes dominant, with a red-shift to 408 nm. The PLE peak of H-aggregates is dissipated, and becomes a weak and broad absorption tail. This phenomenon can be explained in this way: when the concentration is high enough, most of the 3FH form H- and J-aggregates. The emission spectrum at 420 nm mainly originates from J-aggregates because H-aggregation restrains fluorescence and J-aggregation favors fluorescence. This weaker and broader absorption tail demonstrates the fact that the emission at 420 nm slightly originates from H-aggregates, “isolated” chromophores, and

those J-aggregates with a lower aggregation degree. Here, “isolated” chromophores also include those associated molecules if their conjugated backbones are not compact enough (larger than about 1 nm) to exhibit perturbed absorption and emission. The PL emission spectrum has a significant spectral red-shift, and three transition peaks are located at 419, 434, and 459 nm (Figure S1, Supporting Information). Compared with “isolated” chromophores, this emission spectrum of 1 g/L 3FH has red-shifted for 29 nm.

The other oligofluorenes and polyfluorenes also have a similar spectral red-shift effect with increasing concentration, as recorded in Table 1. Compared with the “isolated” chromophores, 3FH, 5FH, 7FH, PFH, and PFO with a concentration of 1g/L have a  $\lambda_{\text{max}}$  red-shift of 52, 43, 43, 41, and 41 nm for PLE spectra. The corresponding PL emission spectra have complex shapes, resulting from a combined interaction of “isolated” chromophores, H- and J-aggregates,

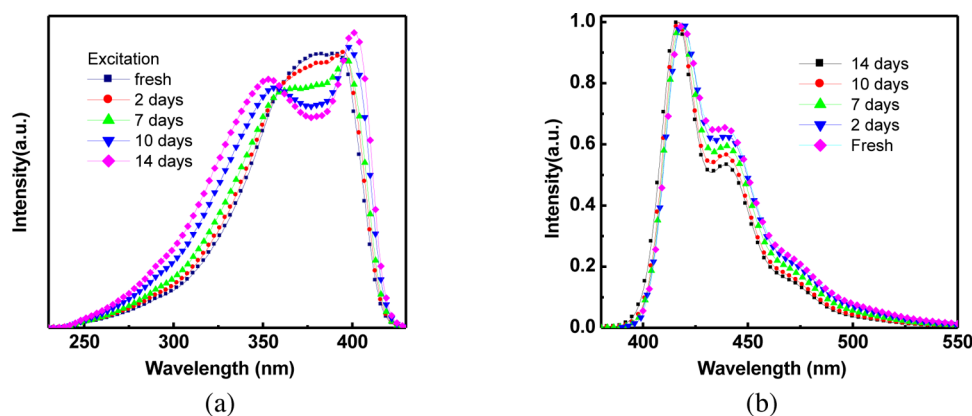


Figure 12. PLE (a) and PL (b) spectra of PFH with different storage times.

together with the reabsorption effect. For PFO with a concentration of 1 g/L, the  $\beta$  phase also adds complexity to the corresponding emission spectra. As Figure 5b shows, the  $\lambda_{\text{max}}$  of 5FH, 7FH, PFH, and PFO is almost located at 440 nm, indicating that the apparent energy shift is above 20 nm for these aggregates. To find out the emission energy shift caused by various molecular structures, the  $\lambda_{\text{max}}$  of the first peak (Table 1) is obtained by peak-fitting with the Gaussian method (Figure 11). Compared with the “isolated” chromophores, 3FH, 5FH, 7FH, PFH, and PFO with a concentration of 1 g/L have a  $\lambda_{\text{max}}$  red-shift of 23, 14, 10, 10, and 10 nm for the first peak of the PL spectra. According to eq 1, polyfluorenes are supposed to have more energy shift because of their longer transition dipole moment, but oligofluorenes with shorter transition dipole moments exhibit larger energy shifts. It suggests that an oligofluorene with a shorter transition dipole moment, such as 3FH, is more flexible and likely to adopt an approximate  $2_1$  helix conformation, and align themselves to form H- or J-aggregates in solutions.

**Time Dependence of Aggregation.** The formation process of H- and J-aggregates is time-dependent. This time dependence is related to the concentration of the oligofluorenes and polyfluorenes. Here PFH was selected to illustrate the time dependence of aggregation. When the concentration is below  $10^{-3}$  g/L, there is no obvious band shift when the storage time increases, indicating that no H- and J-aggregation occurs in the systems. When the concentration of PFH is above  $10^{-3}$  g/L, the PLE spectra change significantly as the storage time increases. Figure 12 shows the PLE and PL emission spectra of PFH solution with a concentration of 0.002 g/L measured after different storage periods. For the PLE spectrum measured right after preparation, the spectral character is the same as that of the  $10^{-3}$  g/L PFH solution, where the maximum absorption band appears at 383 nm. When storing for 20 min, the PLE spectrum exhibits a broad absorption band with the peaks at 383, 362, and 398 nm, which indicates the coexistence of the “isolated” fluorene chromophores, H- and J-aggregates of the chromophores. With the storage time increases, more and more chromophores of PFH form H-aggregates and J-aggregates. As a result, the absorption intensity of “isolated” chromophores decreases, whereas the absorption intensity of aggregates increases. The  $\lambda_{\text{max}}$  of H-aggregates has a blue-shift, and the  $\lambda_{\text{max}}$  of J-aggregates has a red-shift. Meanwhile, the relative intensity of J-aggregates becomes stronger and stronger than that of H-aggregates, since the J-aggregates contribute significantly to the fluorescence. After storing for 8 days, the

spectrum shows that an absorption band at 383 nm decreases, the  $\lambda_{\text{max}}$  of H-aggregates blue-shifts to 360 nm, and the  $\lambda_{\text{max}}$  of J-aggregates red-shifts to 402 nm. With the further increase in the storage time, there is not a significant change with PLE spectra. Therefore, it needs 8 days for 0.002 g/L PFH to form H- and J-aggregates. The corresponding PL spectra show a slight increase of  $I_{440}/I_{417}$  with the increasing storage time presumably due to the formation of H- and J-aggregates, as shown in Figure 12b.

For PFH solution with a higher concentration, the “isolated” chromophores form H- and J-aggregates in a shorter time period after preparation. When the concentration reaches 1 g/L or above, the chromophores form H- and J-aggregates immediately, so the PLE spectrum shows the characteristics of chromophoric aggregates after preparation.

**Site-Selective Fluorescence Spectroscopy.** Site-selective fluorescence spectra obtained for different excited energies are used to investigate the influence of excited energy on the emission. Figure 13 shows the PL emission spectra of 0.01 g/L

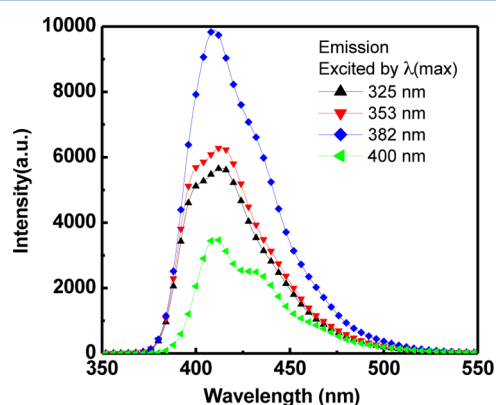
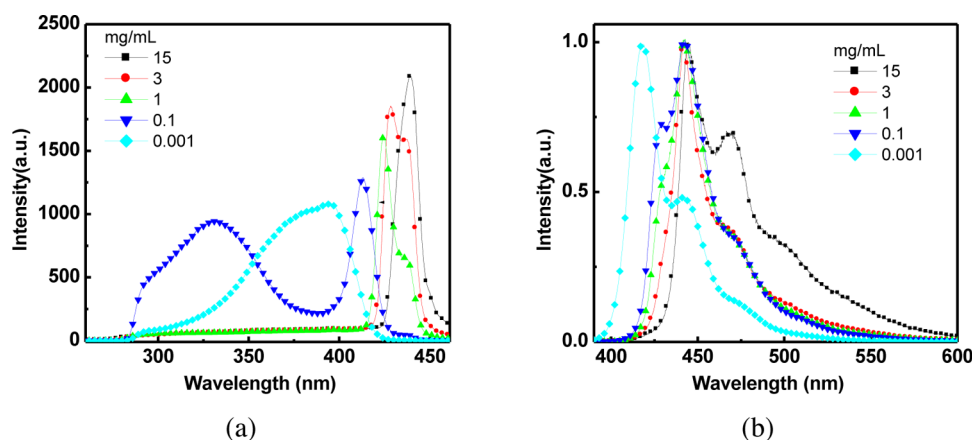


Figure 13. PL spectra of 0.01 g/L PFH excited at different wavelengths.

3FH with different excited energies. 3FH solution with 0.01 g/L has two PLE peaks at 325 nm (H-aggregates) and 382 nm (J-aggregates) (Figure 5b). When excited at 400 (3.00 eV) or 382 nm (3.14 eV), three well-resolved emission bands are observed at 408, 430, and 447 nm, with the one at 408 nm being the strongest peak (Figure S2, Supporting Information). The emission spectrum originating from J-aggregates for the excitation energy is too weak to excite the “isolated” chromophores (required 3.37 eV) and H-aggregates (required



**Figure 14.** (a) PLE spectra (monitored at 470 nm) and PL spectra (excited at 385 nm) of PFO with different concentrations.

3.69 eV). Compared to the emission spectra of “isolated” chromophores shown in Figure 3b, this emission is similar to that of oligofluorenes with longer conjugated length (e.g., 5FH). This result exhibits evidence for the enhancement of the conjugated length due to J-aggregation. The 0–0 transition peak has a spectral blue shift gradually with excited energy increases. When excited at 353 or 325 nm, the transition peaks are located at 398, 413, and 436 nm, respectively (Figure S2, Supporting Information). The spectral shape also exhibits an evident change. This emission spectrum originates from a combined interaction of the “isolated” chromophores, H-aggregates and J-aggregates.

Therefore, this result provides further evidence to confirm that H- and J-aggregation occur in oligofluorene and polyfluorene systems, and J-aggregation has an influence on their conjugated length of chromophores.

**Comparison.** J-aggregates of fluorenes exhibits a  $\beta$ -like  $2_1$  helix conformation, but it is different from the  $\beta$  phase of polyfluorenes noted by Grell et al.<sup>8</sup> The  $\beta$  phase of polyfluorenes is intrachain aggregation of the backbone rings through a fully extended PFO chain segment, adopting the  $2_1$  helix conformation. Tsoi et al. reported that the electronic conjugation length of the  $\beta$  phase is  $30 \pm 12$  monomer units.<sup>47</sup> Oligofluorenes and PFH show no  $\beta$  phase behavior because of limited conjugated length. Among these five molecules, only PFO shows  $\beta$  phase behavior under suitable conditions due to enough conjugation length. Therefore, the PFO  $\beta$  phase can be considered as a special intrachain J-aggregate. The  $\beta$  phase formation in solution also depends on concentration. It is reported that the  $\beta$  phase of PFO only occurs in cyclohexane with a concentration higher than 1 g/L.<sup>8</sup> Figure 14 shows PLE and PL emission spectra of PFO in chloroform with different concentrations. PFO starts to form H- and J-aggregates in chloroform with a concentration at 0.001 g/L. With concentration increases, more and more intramolecular and intermolecular chromophores form H- and J-aggregates. PFO can form the  $\beta$  phase in chloroform only when the concentration is 1 g/L or above. As shown in Figure 11a, when the concentration of PFO reaches 1 g/L, the PLE spectra show a maximum absorption peak at 424 nm and a shoulder peak at 437 nm. The absorption peak at 424 nm originates from J-aggregates, and the shoulder peak confirms the formation of the  $\beta$  phase. Despite the existence of H-aggregates in the system, H-aggregation contributes little to fluorescence and shows a weaker and broader absorption tail on the short-

wavelength side. When the concentration is at 3 g/L, the relative absorption intensity at 437 nm arises. And the  $\lambda_{\max}$  red shifts from 424 to 429 nm, indicating the enhancement of both the  $\beta$  phase and J-aggregates in the system. When the concentration is at 15 g/L, the PLE of J-aggregates has a spectral red-shift from 429 to 440 nm, and the spectrum of the  $\beta$  phase overlaps with that of J-aggregates.

The formation of H- and J-aggregates and the  $\beta$  phase has a great influence on the emission spectra of PFO. As Figure 14b shows, when the concentration is at 0.001 g/L or below, neither H-, J-aggregates nor the  $\beta$  phase forms in this PFO system. The emission spectrum exhibits the typical feature of “isolated” chromophores with the 0–0 transition located at 417 nm, the 0–1 transition located at 440 nm, and the 0–2 transition located at 464 nm. When the concentration is in the range 0.001–1 g/L, the formation of H- and J-aggregates induces the emission red-shift. When the concentration is at 0.001 g/L or above, there are H- and J-aggregates, and the  $\beta$  phase coexists in the system. The emission spectrum exhibits a mixed effect of aggregates and  $\beta$  phase. PL spectra of 1 g/L PFO can be fitted with five separated peaks at about 429, 441, 450, 464, and 495 nm by using the peak-fitting method (Figure S3, Supporting Information). Emission bands at 429 and 450 nm are the 0–0 and 0–1 transition peaks of J-aggregates, which confirms a spectral red-shift to that of “isolated” chromophores. Emission bands at 441, 464, and 495 nm are the 0–0, 0–1, and 0–2 transition peaks of the  $\beta$  phase, respectively. The emission band at 429 nm is supposed to be stronger, but the reabsorption effect depresses this peak due to the small Stokes shift. Here the maximum absorption peak of J-aggregates is at 425 nm, and the emission 0–0 transition peak is at 429 nm. This small Stokes shift induces an emission spectral reabsorption effect. The H-aggregate contributes little to the emission, so it is omitted in this discussion. PL spectra of PFO with a concentration of 3 g/L can be fitted with five separated peaks at about 434, 441, 451, 469, and 500 nm (Figure S3, Supporting Information). The emission bands at 434 and 451 nm are the 0–0 and 0–1 transition peaks of J-aggregates, which are overlapped with the 0–0, 0–1, and 0–2 transition peaks of the  $\beta$  phase at 441, 469, and 500 nm. The emission band at 434 nm is suppressed by the reabsorption effect. Compared to 1 g/L PFO solution, 3 g/L PFO has a stronger emission band at 441 nm because of the relative larger quantity of the  $\beta$  phase in the system.

As noted, the H- and J-aggregates we discussed here are different from excimers which satisfy the Birks definition. For



polyfluorene excimers, the PLE spectrum is the same as the “isolated” chromophores but causes a broad PL emission band in the blue-green spectral region. For H- or J-aggregates, there is a greater absorption blue-shift or red-shift to the PLE spectrum of the “isolated” chromophores. Excimers can form from PFO with higher concentration. PL spectra of 15 g/L PFO can be fitted with five separated peaks at about 444, 454, 467, 495, and 503 nm (Figure S3, Supporting Information). The emission bands at 444 and 467 nm are the 0–0 and 0–1 transition peaks of J-aggregates, which are overlapped with the peaks of the  $\beta$  phase at 444, 467, and 495 nm. The additional peak at 503 nm originates from excimers. Usually the emission of excimers has a lower energy than that of chromophoric aggregates.

Both H- and J-aggregates caused a PL emission band in the blue-green spectral region, but the influence of H- and J-aggregates on the PL emission band is different in nature. J-aggregation favors the fluorescence so that the PL emission band derived from J-aggregates exhibits a higher quantum efficiency, while the emission band H-aggregation presents a lower quantum efficiency.

#### 4. CONCLUSION

We have reported a new idea in presenting the H- and J-aggregation occurring in polyfluorenes and oligofluorenes to understand the influence of chromophore aggregation on photoluminescent emission. Dialkyl-substituted oligofluorenes with different monomer units—3FH, 5FH, and 7FH—and polyfluorenes including PFH and PFO were used to form isolated chromophores and chromophore aggregates in chloroform with different concentrations. A relaxed molecular configuration is simulated to illustrate the spatial arrangement of fluorene bonding configuration. Polyfluorenes and oligofluorenes with this  $2_1$  helical backbone conformation tend to form H- and J-aggregates through strong  $\pi$ – $\pi$  interaction between the backbone rings. These aggregates were induced by a continuous increase of the solution concentration. H- and J-aggregates of polyfluorenes and oligofluorenes show large spectral shifts and distinct changes in band shapes of PLE and PL spectra. This phenomenon is different from what happens with excimers and the  $\beta$  phase. The understanding of H- and J-aggregation behaviors in polyfluorenes and oligofluorenes is important for determining the origin of various red-shifted emissions that occur in blue-emitting polyfluorenes, and developing polyfluorene-based device performance. Ongoing research will focus on investigation of polyfluorene aggregation in dry film conditions as well as some applications of OLEDs and energy conversion.

#### ■ ASSOCIATED CONTENT

##### Supporting Information

The synthesis procedures and analytical data of PF<sub>6</sub>, PFO EO<sub>3</sub>, and oligofluorene OF<sub>6</sub>. This material is available free of charge via the Internet at <http://pubs.acs.org>.

#### ■ AUTHOR INFORMATION

##### Corresponding Authors

\*E-mail: [yhdeng@scut.edu.cn](mailto:yhdeng@scut.edu.cn).

\*E-mail: [gliu@lbl.gov](mailto:gliu@lbl.gov). Phone: +1-510-486-7207. Fax: +1-510-486-7303.

##### Notes

The authors declare no competing financial interest.

#### ■ ACKNOWLEDGMENTS

This project is sponsored by the U.S. Department of Energy's Building Technologies (BT) Program and the National Energy Technology Laboratory.

#### ■ REFERENCES

- (1) Neher, D. Polyfluorene Homopolymers: Conjugated Liquid-Crystalline Polymers For Bright Blue Emission And Polarized Electroluminescence. *Macromol. Rapid Commun.* **2001**, *22*, 1366–1385.
- (2) Honmou, Y.; Hirata, S.; Komiyama, H.; Hiyoshi, J.; Kawachi, S.; Iyoda, T.; Vacha, M. Single-Molecule Electroluminescence And Photoluminescence Of Polyfluorene Unveils The Photophysics Behind The Green Emission Band. *Nat. Commun.* **2014**, *5*, No. 4666.
- (3) Knaapila, M.; Monkman, A. P. Methods For Controlling Structure And Photophysical Properties In Polyfluorene Solutions And Gels. *Adv. Mater.* **2013**, *25*, 1090–1108.
- (4) Chen, S. H.; Su, A. C.; Su, C. H.; Chen, S. A. Phase Behavior Of Poly(9,9-Di-N-Hexyl-2,7-Fluorene). *J. Phys. Chem. B* **2006**, *110*, 4007–4013.
- (5) Chen, S. H.; Su, A. C.; Su, C. H.; Chen, S. A. Crystalline Forms And Emission Behavior Of Poly(9,9-Di-N-Octyl-2,7-Fluorene). *Macromolecules* **2005**, *38*, 379–385.
- (6) Chen, S. H.; Su, A. C.; Chen, S. A. Noncrystalline Phases In Poly(9,9-Di-N-Octyl-2,7-Fluorene). *J. Phys. Chem. B* **2005**, *109*, 10067–10072.
- (7) Grell, M.; Bradley, D. D. C.; Long, X.; Chamberlain, T.; Inbasekaran, M.; Woo, E. P.; Soliman, M. Chain Geometry, Solution Aggregation And Enhanced Dichroism In The Liquid-Crystalline Conjugated Polymer Poly(9,9-Dioctylfluorene). *Acta Polym.* **1998**, *49*, 439–444.
- (8) Grell, M.; Bradley, D. D. C.; Ungar, G.; Hill, J.; Whitehead, K. S. Interplay Of Physical Structure And Photophysics For A Liquid Crystalline Polyfluorene. *Macromolecules* **1999**, *32*, 5810–5817.
- (9) Jia, Z.; Yuan, W.; Zhao, H.; Hu, H.; Baker, G. L. Composite Electrolytes Comprised Of Poly(Ethylene Oxide) And Silica Nanoparticles With Grafted Poly(Ethylene Oxide)-Containing Polymers. *RSC Adv.* **2014**, *4*, 41087–41098.
- (10) Babel, A.; Jenekhe, S. A. Electron Transport In Thin-Film Transistors From An N-Type Conjugated Polymer. *Adv. Mater.* **2002**, *14*, 371–374.
- (11) Gong, X. O.; Iyer, P. K.; Moses, D.; Bazan, G. C.; Heeger, A. J.; Xiao, S. S. Stabilized Blue Emission From Polyfluorene-Based Light-Emitting Diodes: Elimination Of Fluorenone Defects. *Adv. Funct. Mater.* **2003**, *13*, 325–330.
- (12) Prieto, I.; Teetsov, J.; Fox, M. A.; Bout, D. A. V.; Bard, A. J. A Study Of Excimer Emission In Solutions Of Poly(9,9-Dioctylfluorene) Using Electrogenated Chemiluminescence. *J. Phys. Chem. A* **2001**, *105*, 520–523.
- (13) Winnik, F. M. Photophysics Of Preassociated Pyrenes In Aqueous Polymer-Solutions And In Other Organized Media. *Chem. Rev.* **1993**, *93*, 587–614.
- (14) Spano, F. C.; Silva, C. H- And J-Aggregate Behavior In Polymeric Semiconductors. *Annu. Rev. Phys. Chem.* **2014**, *65*, 477–500.
- (15) Bliznyuk, V. N.; Carter, S. A.; Scott, J. C.; Klarner, G.; Miller, R. D.; Miller, D. C. Electrical And Photoinduced Degradation Of Polyfluorene Based Films And Light-Emitting Devices. *Macromolecules* **1999**, *32*, 361–369.
- (16) Philpott, M. R.; Lee, J. W. Exciton Theory Of The Excited Electronic States Of Coupled Molecular Aggregates. *J. Chem. Phys.* **1972**, *57*, 2026–2033.
- (17) Mcrae, E. G.; Kasha, M. Enhancement Of Phosphorescence Ability Upon Aggregation Of Dye Molecules. *J. Chem. Phys.* **1958**, *28*, 721–722.
- (18) Vekshin, N. L. Screening Hypochromism Of Biological Macromolecules And Suspensions. *J. Photochem. Photobiol., B* **1989**, *3*, 625–630.

- (19) Banerji, N. Sub-Picosecond Delocalization In The Excited State Of Conjugated Homopolymers And Donor-Acceptor Copolymers. *J. Mater. Chem. C* **2013**, *1*, 3052–3066.
- (20) Barford, W. Excitons In Conjugated Polymers: A Tale Of Two Particles. *J. Phys. Chem. A* **2013**, *117*, 2665–2671.
- (21) Moliton, A.; Hiorns, R. C. Review Of Electronic And Optical Properties Of Semiconducting Pi-Conjugated Polymers: Applications In Optoelectronics. *Polym. Int.* **2004**, *53*, 1397–1412.
- (22) Deng, Y. H.; Li, Y. B.; Wang, X. G. Colloidal Sphere Formation, H-Aggregation, And Photoresponsive Properties Of An Amphiphilic Random Copolymer Bearing Branched Azo Side Chains. *Macromolecules* **2006**, *39*, 6590–6598.
- (23) Li, Y. B.; Deng, Y. H.; Tong, X. L.; Wang, X. G. Chromophore H-Aggregation Kinetics Of A Branched Side-Chain Azo Polyelectrolyte. *Acta Polym. Sin.* **2005**, 834–839.
- (24) Deng, Y. H.; Wang, X. G. H-Aggregation And Photo-Responsive Behavior Of An Azo Polyelectrolyte. *Acta Polym. Sin.* **2003**, 704–708.
- (25) Deng, Y. H.; Wang, X. G. Ph Effects On H-Aggregation Of Photo-Responsive Azo Polyelectrolytes. *Acta Polym. Sin.* **2003**, 709–713.
- (26) Deng, Y. H.; Tuo, X. L.; Cheng, H.; Wang, X. G. Synthesis And H-Aggregation Of A Novel Polyelectrolyte Bearing Branched Azo Side Chains. *Chem. J. Chin. Univ.* **2003**, *24*, 1320–1324.
- (27) Gui, R.; Wan, A.; Liu, X.; Yuan, W.; Jin, H. Water-Soluble Multidentate Polymers Compactly Coating Ag<sub>2</sub>S Quantum Dots With Minimized Hydrodynamic Size And Bright Emission Tunable From Red To Second Near-Infrared Region. *Nanoscale* **2014**, *6*, 5467–5473.
- (28) Hu, H.; Yuan, W.; Zhao, H.; Baker, G. L.; Novel, A. Polymer Gel Electrolyte: Direct Polymerization Of Ionic Liquid From Surface Of Silica Nanoparticles. *J. Polym. Sci., Part A: Polym. Chem.* **2014**, *52*, 121–127.
- (29) Monahan, A. R.; Blossey, D. F. Aggregation Of Arylazonaphthols. I. Dimerization Of Bonadur Red In Aqueous And Methanolic Systems. *J. Phys. Chem.* **1970**, *74*, 4014–4021.
- (30) Monahan, A. R.; Germano, N. J.; Blossey, D. F. Aggregation Of Arylazonaphthols. II. Steric Effects On Dimer Structure In Water. *J. Phys. Chem.* **1971**, *75*, 1227–1233.
- (31) Tinoco, I. Hypochromism In Polynucleotides. *J. Am. Chem. Soc.* **1960**, *82*, 4785–4790.
- (32) Bolton, H. C.; Weiss, J. J. Hypochromism In Ultra-Violet Absorption Of Nucleic Acids And Related Structures. *Nature* **1962**, *195*, 666–668.
- (33) Meinardi, F.; Cerminara, M.; Sassella, A.; Bonifacio, R.; Tubino, R. Superradiance In Molecular H Aggregates. *Phys. Rev. Lett.* **2003**, *91*, No. 247401.
- (34) Wang, Y. Resonant 3rd-Order Optical Nonlinearity Of Molecular Aggregates With Low-Dimensional Excitons. *J. Opt. Soc. Am. B* **1991**, *8*, 981–985.
- (35) Misawa, K.; Ono, H.; Minoshima, K.; Kobayashi, T. New Fabrication Method For Highly Oriented J-Aggregates Dispersed In Polymer-Films. *Appl. Phys. Lett.* **1993**, *63*, 577–579.
- (36) Grad, J.; Hernandez, G.; Mukamel, S. Radiative Decay And Energy-Transfer In Molecular Aggregates - The Role Of Intermolecular Dephasing. *Phys. Rev. A* **1988**, *37*, 3835–3846.
- (37) Steinhoff, R.; Chi, L. F.; Marowsky, G.; Mobius, D. Protonation And Monolayer Aggregation Studied By 2nd-Harmonic Generation. *J. Opt. Soc. Am. B* **1989**, *6*, 843–847.
- (38) Yuan, W.; Zhao, H.; Hu, H.; Wang, S.; Baker, G. L. Synthesis And Characterization Of The Hole-Conducting Silica/Polymer Nanocomposites And Application In Solid-State Dye-Sensitized Solar Cell. *ACS Appl. Mater. Interfaces* **2013**, *5*, 4155–4161.
- (39) Yuan, W.; Zhao, H.; Baker, G. L. Low Glass Transition Temperature Hole Transport Material In Enhanced-Performance Solid-State Dye-Sensitized Solar Cell. *Org. Electron.* **2014**, *15*, 3362–3369.
- (40) Hu, H.; Yuan, W.; Lu, L.; Zhao, H.; Jia, Z.; Baker, G. L. Low Glass Transition Temperature Polymer Electrolyte Prepared From Ionic Liquid Grafted Polyethylene Oxide. *J. Polym. Sci., Part A: Polym. Chem.* **2014**, *52*, 2104–2110.
- (41) Klaerner, G.; Miller, R. D. Polyfluorene Derivatives: Effective Conjugation Lengths From Well-Defined Oligomers. *Macromolecules* **1998**, *31*, 2007–2009.
- (42) Wasserberg, D.; Dudek, S. P.; Meskers, S. C. J.; Janssen, R. A. J. Comparison Of The Chain Length Dependence Of The Singlet- And Triplet-Excited States Of Oligofluorenes. *Chem. Phys. Lett.* **2005**, *411*, 273–277.
- (43) Jo, J. H.; Chi, C. Y.; Hoger, S.; Wegner, G.; Yoon, D. Y. Synthesis And Characterization Of Monodisperse Oligofluorenes. *Chem.—Eur. J.* **2004**, *10*, 2681–2688.
- (44) Fukuda, M.; Sawada, K.; Yoshino, K. Synthesis Of Fusible And Soluble Conducting Polyfluorene Derivatives And Their Characteristics. *J. Polym. Sci., Polym. Chem.* **1993**, *31*, 2465–2471.
- (45) Dewar, M. J. S.; Zuebis, E. G.; Healy, E. F.; Stewart, J. J. P. The Development And Use Of Quantum-Mechanical Molecular-Models 0.76. Am1 - A New General-Purpose Quantum-Mechanical Molecular-Model. *J. Am. Chem. Soc.* **1985**, *107*, 3902–3909.
- (46) Kasha, M.; Rawls, H. R.; Ashraf El-Bayoumi, M. The Exciton Model In Molecular Spectroscopy. *Pure Appl. Chem.* **1965**, *11*, 371–392.
- (47) Tsoi, W. C.; Charas, A.; Cadby, A. J.; Khalil, G.; Adawi, A. M.; Iraqi, A.; Hunt, B.; Morgado, J.; Lidzey, D. G. Observation Of The Beta-Phase In Two Short-Chain Oligofluorenes. *Adv. Funct. Mater.* **2008**, *18*, 600–606.